STM JOURNALS

International Journal of
Algorithms Design and
Analysis Review

ISSN: 2584-1866
Volume 2, Issue 1, 2024
January—June
DOI (Journal): 10.37591/IJADAR

https://journals.stmjournals.com/ijadar

Review IJADAR

Human Deep Skin Surface Vibration Frequency Detection from CT and DT Signals Using Genetic Algorithms

Narasimha Chary Ch[1,]*, CH. GVN Prasad[2]

Abstract

To diagnose respiratory problems early on, a contactless, non-invasive, real-time assessment of human vibration is a crucial prerequisite. Optoelectronic plethysmography (OEP) and the forced oscillation technique (FOT), are two widely utilized methodologies, depending on variations in each patient's local chest impedance. Calibration of the devices before each measurement is hence the primary problem of these approaches. This report presents a simulation-based analysis to assess the effectiveness of the CT and DT Signals as a substitute. The study's conclusion suggested that the self-mixing-based optical feedback interferometry (SM-OFI) might be employed as a vibration measurement tool. The outcomes also show that CT and DT Signals can detect heart activity. One of the main goals of clinical research and science is to determine vibration perception thresholds (VPT) to evaluate human somatosensory capabilities. Seldom has the reaction of several mechanoreceptors to a growing contact force been investigated. We hypothesize that the VPTs of fast-adapting mechanoreceptors in the human foot sole drop as contact force increases. Using a vibration exciter, the VPTs of ten healthy volunteers were recorded at 30 Hz and 200 Hz at the right foot's heel. An integrated force sensor allowed for the exact adjustment of contact forces within the range of 0.3 N to 9.6 N. Contact force and frequency were found to have significant major effects. Additionally, a significant relationship was seen between frequency and contact force, indicating that an increase in contact force had an impact. We assume that the Meissner and Pacinian corpuscles follow the same rules for contrast enhancement and spatial summation, respectively. Because Pacinian corpuscles are located in the periosteum or interosseous membrane, we assume that they have an impact on them in addition to spatial summation.

Keywords: Meissner and Pacinian corpuscles, self-mixing effect, evolutionary approach, vibrations measuring, visual output interferometry, diagnostic instrument

***Author for Correspondence**
Narasimha Chary Ch
E-mail: narasimhachary.dr@gmail.com

[1]Associate Professor, Department of Computer Science and Engineering, Sri Indu College of Engineering & Technology, Sheriguda, Telangana, India
[2]Professor, Department of Computer Science and Engineering, Sri Indu College of Engineering & Technology, Sheriguda, Telangana, India

Received Date: April 10, 2024
Accepted Date: April 30, 2024
Published Date: May 30, 2024

Citation: Narasimha Chary Ch, CH. GVN Prasad. Human Deep Skin Surface Vibration Frequency Detection from CT and DT Signals Using Genetic Algorithms. International Journal of Algorithms Design and Analysis Review. 2024; 2(1): 9–16p.

INTRODUCTION

The breathing cycle causes the surface of the human body to vibrate. There is clinically significant information about respiratory illnesses contained in these vibrations. For the measurement, conventionally minimally intrusive techniques like optoelectronic plethysmography (OEP) [1] and forced oscillation technique (FOT) [2] are employed. The local chest impedance variation brought about by the mechanical characteristics of the several tissues that make up the chest wall and lung parenchyma is the basis for these measuring systems [3]. For this reason, before running the test, each instrument needs to be calibrated individually.

To attain the lowest impedance level necessary for an accurate measurement, the individuals are also recommended to breathe deeply while being tested. This work investigates the possible applications of self-mixing-based optical feedback interferometry (OFI) through a simulation-based analysis.

All types of lasers, including quantum dots, gas, solid state, semiconductors, and vertical-cavity surface-emitting lasers (VCSELs), exhibit the self-mixing effect when they are subjected to a back reflection from a distant surface [4]. The SM-OFI signal is an interferometry signal that takes the shape of the laser's modulated resonant power. Furthermore, the resonant power of an SM-OFI laser beam is regulated in accordance with the displacement of the vibrating surface. The vibration frequency is typically extracted using the fringes counting approach; nevertheless, there is an ongoing discussion on the counting method's accuracy in the context of clinical measurement. Therefore, a genetic algorithm (GA) was used to process the signal to automate the measuring process. The GA gets better. The study's result indicated that the benefits of both GA and SM-OFI will open the door for the creation of new diagnostic instruments. Additionally, this instrument will be useful for the clinical assessment of many respiratory conditions, including asthma, chronic obstructive lung disease, and the efficacy of bronchodilator medications.

The term human vibrating is the impact of the environment's mechanical vibrations on the human body. We have access to a variety of vibration sources in our daily lives, such as such found in cars, trains, and buses. During every minute of their day at work, a lot of individuals are subjected to other vibrations.

METHODS

SM-OFI

The self-mixing effect is an effect that modifies the laser diode's electrical field based on the target's partially reflected light [5]. As a result, the back-reflected optical power produces an interferometric signal [6]. All types of lasers, including quantum dots, gas, solid state, semiconductors, and VCSELs, exhibit the self-mixing effect, which is a universal phenomenon [7]. The SM-OFI signal bears an accompanying calculation [8].

Participants

In total, 41 participants in 10 age groups, ranging in age from 20 to 77 years old, were in good health and engaged with the studies (median ± median absolute deviation: 44.8 ± 16.7 years). The participants met the conditions as follows: they were all right-handed Japanese women without psychiatric disorders, without major skin injury such as severe sunburn, without physical disabilities, and without being pregnant or nursing. Respondents submitted written informed consent to participate in the study after being made aware of its goal. The experiment's participants were told they could end it whenever they wanted to. This study was authorized by the Ethics Committee of the Shiseido Research Center, and all operations followed the established guidelines.

Equipment

We made use of a previously created apparatus that concurrently monitors skin deformation and applies quantitative suction stimulation to the skin. The air in an air cylinder is compressed and expanded by a voice-coil linear actuator (H2W Technologies, VMS30-090-LB-1) (SMC, MQQLL30-100DM). Via an air tube, the oscillations are conveyed to the contactor, whereupon suction pressure stimulates the skin through the contactor's suction hole.

The contractor has a 2 mm diameter suction hole in the center. During the measurements, a spring-loaded contact force adjustment mechanism maintains a constant pressing force on the skin. The skin deformation produced by suction stimulation was measured using a 2D laser displacement sensor (Keyence LJ-V7080) installed inside the contactor and transmitted laser light. Figure 1 shows the altered shape of the skin on the laser's irradiation line at the suction hole. To be able to measure the pressure exerted on the cheek, a pressure sensor (PISCO, VUS11-AR) was connected to the air tube.

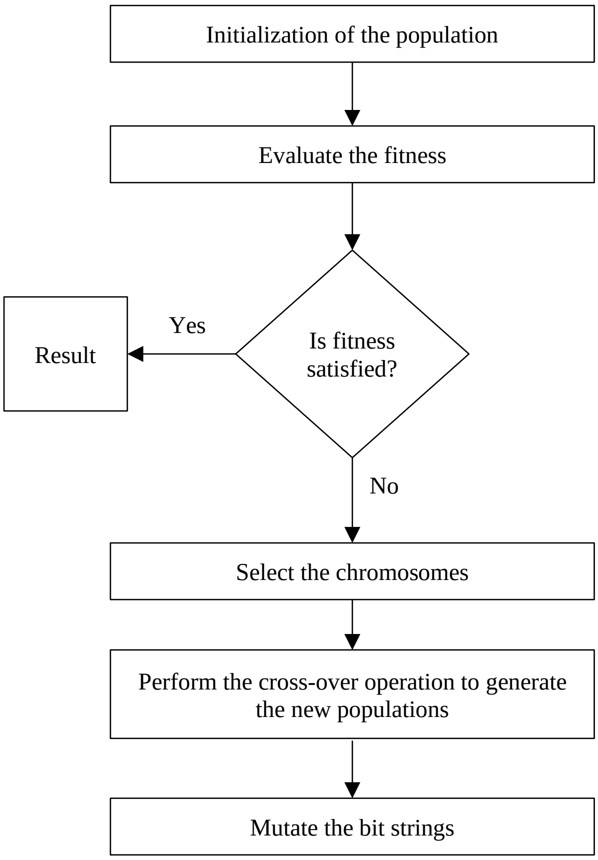

Figure 1. Flow chart of the genetic algorithm.

Assessment of Stimulus Thresholds

Using psychophysical techniques, we assessed the participant's tactile impression of negative pressure on their cheeks statistically. A room with a consistent temperature of 22.0°C and a relative humidity of 45.0% was used for the investigation. We used a pen to mark the stimulation point on the left cheek, which was the point where the stimulator made contact with the skin, following a 15-minute acclimation period and the participant's first face wash with facial washing foam. Initially, the subject was instructed to rest their face on a chin rest while maintaining a steady cheek position—the stimulation point. When the stimulus was perceived, the participant was instructed to raise their hands.

The person who established the stimulation threshold was. By adaptively shifting the step of the displayed stimulus based on the participant's reactions, this method decreases the number of measurements while boosting the accuracy of the stimulus threshold measurements. The following four rules created a basis for the method that was employed for evaluating stimulus change: The change step width was (1) halved when the stimulus step's direction of change was reversed, (2) held constant when the stimulus step's direction of change remained constant, (3) doubled when the stimulus step's direction of change remained constant three times in a row, and (4) boosted when the stimulus step's direction of change remained constant twice in a row. The third step width measurement was kept constant and was not doubled if the stimulus step width doubling that happened right before the current stimulus step was the reason behind the reversal of the step direction. Nevertheless, the third change step width was doubled if the reversal that occurred just before the current stimulus step was not brought on by double the stimulus step change. We chose 10 Hz oscillation stimuli since it is well known that the skin replies to these more readily than it does to steady-state stimuli.

We investigated a wide variety of tactile sensory traits in patients from 20 to 77 years of age using the same index without causing participant pain by employing dynamic vibrating stimuli, which are easier to recognize than static stimuli. The stimulus duration was 3.5 s, and within that time frame, 10 Hz stimulation was given for 2.0 s (Figure 2). The range of stimulus intensity was set from −0.05 to −13.5 kPa. The measurement started at the largest stimulus intensity of −13.5 kPa. If the subject perceived the stimulus, the stimulus intensity was reduced; if not, the stimulus intensity was increased. The measurement ended when the step fluctuation was less than 0.1 kPa or when the upper or stimulus intensity limit was presented three consecutive times. The last stimulus to be provided served as the stimulus threshold if, after a maximum of thirty trials, the step fluctuation range did not converge. All the participants underwent the measurements three times. The three trials were carried out by adjusting the interval time and the stimulus presentation point on the cheek by 5 mm to account for the impact of skin fatigue brought on by repeated stimulation on the mechanical characteristics of the skin. At least five minutes passed between trials. Prior to the test, practice trials were carried out, and measurements were taken once the participants had a complete understanding of the stimulation process.

The skin surface in this early model was considered to be smooth. Thus, the fingerprints or epidermal ridges that define monkeys' digital skin are ignored in this method. Although the exact mechanism behind the enhanced tactile sense has long been proposed these surface microstructures continue to be poorly understood. Six The evolution of artificial and numerical fingertip models in recent years has made it possible to learn how these wavy features alter the skin's stress distribution. These studies provided strong support for an earlier theory by Cauna that suggested an arm-lever-like effect on every person's epidermal ridge, amplifying the subcutaneous strain.

However, the mechanoreceptor terminal must lie precisely in relation to the epidermal ridge and somewhat close to the skin's surface for this stress-concentrating process to occur. This is true for the deeper Pacinian corpuscles, which are involved in the coding of finer textures (lateral size below approximately 200 µm), but not for the SA1 receptors, which govern the perception of coarse textures.

ASSESSMENT OF SKIN DEFORMITY

Throughout the stimulus threshold measurements, skin deformation brought on by suction stimulation was measured using a two-dimensional laser displacement meter (Keyence LJ-V7080) installed inside the contactor. In this investigation, we employed skin deformation data at the suction hole center to determine the skin deformation along the suction hole's laser irradiation line. The skin deformation observed just before the onset of suction was used as the zero reference in the calculation of these results. A skin deformation index was calculated by averaging the five local maxima of skin deformation (peak skin deformation) at the middle of the region where 10 Hz suction oscillation stimulation was applied. When the same amount of negative pressure was provided in each threshold measurement during the initial stimulus presentation, the peak skin deformation was computed from the data. With each threshold measurement in the PEST approach, the stimulus quantity and the number of presentations varied. Thus, we could compare skin properties across trials without the influence of stimulus strength or skin exhaustion from repetitive stimulus presentation by comparing the peak skin deformation at the initial stimulus presentation.

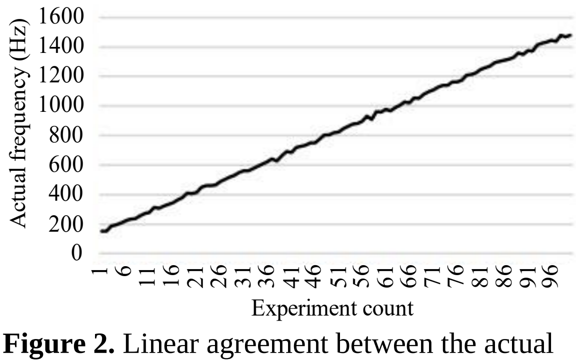

Figure 2. Linear agreement between the actual and estimated vibration frequency.

Analysis

The measured skin deformation and negative pressure data were processed by MATLAB software. The correspondence between skin deformation and tactile perception was examined for each trial, as the skin response to the stimulus may differ for each trial. When the intrarater reliability was confirmed for repeated measurements, a linear mixed analysis approach was used. Intrarater reliabilities for the stimulus threshold and peak skin deformation were estimated using intra-class correlation coefficients (ICCs). To determine the ICC scores, the degree of score consistency for the same subject over three times was examined using a two-way random model. Values were regarded as indicative of intra-participant dependability when the residual $\chi 2$ value analysis of the null model with no explanatory variables was significant and the ICC was greater than.50 (considered moderate reliability). In such cases, a linear mixed model using the maximum likelihood method was used. Age or peak skin deformation was added as a fixed variable, and participants were added to the model as random effects. To investigate how the explanatory factors affected the stimulus threshold or peak skin deformation, likelihood ratio tests using the null model were performed. Different models were employed to study the effects of age and skin deformation. The significance probability was set at 5%. The statistical software R (version 4.1.3) was employed in the processing.

However, we have proposed in recent research that fingerprints might play a different role in the perception of fine textures. The quick skin vibrations that are produced when actively scanning the fingertip over the surface act as a mediator for this impression. It has been demonstrated that the interfacial stress field between the skin and the substrate is spatially modulated by the existence of epidermal ridges. This therefore causes the subcutaneous skin vibrations caused by period-like textural elements to be amplified, much like the ridges themselves. As is the case for PCs, this mechanism necessitates a mechanoreceptor receptive field that is far bigger than the inter-ridge duration. The fingerprint pattern is merely marginally dependent on the placement of the mechanoreceptor. Furthermore, as long as the ridges are (1) deep enough to cause significant interfacial stress modulations and (2) oriented perpendicular to the scanning axis, the precise profile of the ridges should not matter. A biomimetic sensor that simulates the functioning of a single PC in the fingertip was used to illustrate this mechanism. Whether the mechanism demonstrated by this idealistic apparatus applies to a real fingertip is one reasonable question. Technically speaking, answering this question is difficult because there is currently no means to gauge the stress that mechanoreceptors endure in an actual digit. On the other hand, variations in the global friction force pressing on the finger during tactile exploration should be expected to manifest as variations in texture-induced subcutaneous vibrations. Recent research based on this concept quantifies the local skin vibrations at the fingertip when the finger is scanned across different textured materials using a displacement probe. Through independent psychophysical investigations, the intensity of these vibrations, weighted by the PCs' spectral sensitivity, might be associated with the experience of roughness.

$$P(\tau) = Po\ [1 + mI(\tau)] \quad (1)$$

Where, m is the modulation index, I(τ) is the interference function that represents the self-mixing effect on the emitted optical intensity, P(τ) is the emitted optical power under external feedback, Po is the free-running optical power, and $\phi \boldsymbol{R}\ (\tau)$ and $\phi O\ (\tau)$ are the optical phase functions that are indicated under and without feedback, respectively.

$$(\tau) = (\phi F\ (\tau)) \quad (2)$$

$$\phi F\ (\tau) = \phi 0\ (\tau) - [\phi F\ (\tau) + \mathrm{a}\ \tan(\alpha)] \quad (3)$$

$$\phi 0\ (\tau) = 4\pi L/\lambda o \quad (4)$$

Where, m is the modulation index, I(τ) is the interference function that represents the self-mixing effect on the emitted optical intensity, P(τ) is the emitted optical power under external feedback, Po is the free-running optical power, and $\phi \boldsymbol{R}\ (\tau)$ and $\phi O\ (\tau)$ are the optical phase functions that are indicated under and without feedback, respectively.

Genetic Algorithm

An optimization method called a genetic algorithm looks for the extrema points for a particular objective function. The algorithm is constructed in such a way as to replicate the selection process that natural-biological evolution follows [9]. Natural phenomenon also enriches the algorithm. Consequently, the objective function's variables are regarded as chromosomes. Therefore, by carrying out the various updating activities on the chromosomes—such as selection, which controls the generation, crossover, which creates the generation, and mutation, which improves the generation quality—an ideal solution is reached [10]. The flowchart illustrating the genetic algorithm's functionality is displayed in Figure 1.

Objective Function

The search for the positions of zeros in the function derivatives is derived mathematically from the objective function. In the immediate region, these zero locations result in a minimal value. As a result, an optimal value is the total best-fit value among various local values. Vibrations are primarily the periodic change in the equilibrium position. This recurring change in the target's position forces the laser's resonant mode to switch to a different dominant mode. Consequently, vibrations are regarded as a harmonic fluctuation in the exterior cavity's length, which may be mathematically represented as follows:

$$(\tau) = Lo + \Delta L \cos(2\pi f\tau + \theta o) \quad (5)$$

where Lo and ΔL are the equilibrium position and the amplitude of the vibration, respectively, and θo denotes the initial phase of the emission [11]. Hence, the objective function in such a case, is represented as

$$(fest) = \sum [Ff\ (\tau) - Ff\ (\tau, fest)]\ 2\ n\ i=1 \quad (6)$$

where, Ff(τ) is the time-varying observed signals. Ff (τ, fest) is the estimated signal processed over 'n' sampling points.

RESULTS AND DISCUSSION

Under normal light physiological stress situations, the human body's plethysmogram normally has higher frequency components between 1 Hz and 1.5 Hz [12]. A few lower frequency components are also present, which are responsible for heart activity. As a result, the genetic algorithm-based SM-OFI simulation's vibration frequency mimic spans from 100 Hz to 2 kHz. In turn, this range allows for the simulation of both activities. Table 1 contains a list of the parameters used in the simulation environment. With a mutation and crossover probability of 0.5 and 0.8, respectively, the population size was limited to 200. Table 1 contains a list of the parameters used in the simulation environment. With a mutation and crossover probability of 0.5 and 0.8, respectively, the population size was limited to 200. Additionally, the maximum generation was limited to fifty. Thirty experiments were conducted to produce thirty solutions. The best statistical performance was used to estimate the final values. Table 2 lists the statistical characteristics of three frequencies: 150 Hz, 900 Hz, and 1.5 kHz. For the various vibration frequency values, a total of 100 trials were conducted to assess the evolutionary algorithm's repeatability. The experimental results are shown in Figure 2, which supports the linear relationship with a curve fitting of 0.93R 2 between the measured and actual vibrations.

Table 1. Parameters used in genetic algorithms.

Parameters	Value
Population size	200
Crossover probability	0.8
Initial mutation probability	0.5
Maximum generation	50

Table 2. Statistical results were obtained from three different frequencies.

Statical parameters	150 Hz	900 Hz	1.5 kHz
Mean	149.85	899.90	1.50
Variance	0.04	0.13	0.00
Standard deviation	0.21	0.36	0.04

Using a biomimetic technique, this straightforward biomechanical experiment verifies the applicability of the spectral amplification process described in reference 14 for human touch perception. It demonstrates that the range of skin vibrations evoked during tactile exploration is largely determined by the relative orientation of the scanning axis and the fingerprints in contact with the surface. According to this research, comparing radial and distal scanning orientations offers a quick and easy method to evaluate how fingerprints influence texture-induced skin vibrations.

The same approach could be similarly implemented in neuro- or psychophysical experiments. As previously mentioned, skin characteristics affect tactile perception. It is often known that each person has different physical characteristics for their skin, particularly the loss of suppleness and extensibility with age.

Therefore, skin's physical properties contribute to individual differences in tactile perception. Though the skin is believed to influence tactile perception, it is still unknown how the various physical characteristics of skin influence tactile perception. Clarifying the contribution of skin's physical properties to tactile perception can improve our understanding of tactile perception mechanisms. As a result, more accurate correlations between tactile perception and widely differing objective stimuli can be found, and by taking good care of the skin, tactile perception—which deteriorates with age—can be preserved or even enhanced. Unfortunately, it has not been able to demonstrate how the physical characteristics of the skin affect tactile perception since it is difficult to detect the deformation of the skin in response to mechanical stimuli.

CONCLUSION

Based on the SM-OFI Technique, the genetic algorithm approach-based simulation result shows a linear agreement between the estimated and actual vibration frequency. Therefore, SM-OFI using a genetic algorithm has demonstrated its capacity to extract the SM-OFI Technique, the genetic algorithm approach-based simulation result shows a linear agreement between the estimated and actual vibration frequency. Vibration frequency from human skin to detect any respiratory illness, based on the statistical analysis and simulation result. The SM-OFI that uses a genetic algorithm has reasonable linearity over a broad frequency range of 100 Hz–2 kHz. The method also fits excellently while measuring heart activity.

REFERENCES

1. Trupthi M, Narasimha Chary CH, Sneha S, et al. LCDDF: An adaptive and learning-based framework with feature selection for efficient detection of concept drift in data streams. 2024 Feb 1 [Preprint]. 1st version available from Research Square. DOI: 10.21203/rs.3.rs-3893993/v1.
2. Rovati L, Cattini S, Palanisamy N. Measurement of the fluid-velocity profile using a self-mixing superluminescent diode. Meas Sci Technol. 2011;22(2):025402. DOI: 10.1088/0957-0233/22/2/025402.
3. Milesi I, Norgia M, Pompilio PP, Svelto C, Dellaca RL. Measurement of local chest wall displacement by a custom self-mixing laser interferometer. IEEE Trans Instrum Meas. 2011;60(8):2894–2901. DOI: 10.1109/TIM.2011.2118830.
4. Prashanthi J, Santhoshi TS, Goud KR, Chary N. IoT security protocols for multimodal biometric system-based identification of individual vault access. Int J Comput Tech. 2024;11(1):159–162.

5. Bhushan PV, Chary CN, Nithesh V, Singh R. An efficient system for heart risk detection using associative classification and genetic algorithms. Int J Comput Tech. 2017 Nov-Dec;4(6):131–139.
6. Bhushan PV, Nitesh V, Chary CN, Gupta KG. Novel approach for multi-cancers prediction system using various data mining techniques. Int J Manag Technol Eng. 2018 Aug;8(VIII):1629–1640.
7. Li J, Niu H, Niu Y. Laser feedback interferometry and applications: a review. Opt Eng. 2017;56:050901. DOI: 10.1117/1.OE.56.5.050901.
8. Ramírez-Miquet EE, Perchoux J, Da Costa Moreira R, Luna-Arriaga A, Zhaoa Y, Tronche C, Sotolongo-Costa O. Optical feedback interferometry: from basics to applications of laser flowmetry. Rev Cuba Fis. 2017;34:48-57.
9. Gupta G, Narasimha Chary C, Krishna A. Study on health care life log by the level of care required using keygraph technology in text data mining. J Innov Dev Pharm Tech Sci. 2018;1(1):22–27.
10. Haupt RL, Haupt SE. Practical genetic algorithms. 2nd ed. Hoboken, NJ, USA: John Wiley & Sons, Inc.; 2003.
11. Stetson KA. Method of vibration measurements in heterodyne interferometry. Opt Lett. 1982;7:233–234. DOI: 10.1364/ol.7.000233.
12. Yuan H, Poeggel S, Newe T, Lewis E, Viphavakit C, Leen G. An experimental study of the effects of external physiological parameters on the photoplethysmography signals in the context of local blood pressure (hydrostatic pressure changes). Sensors (Basel). 2017;17: DOI: 10.3390/s17030556.

